Chemical Engineering Journal 165 (2010) 980–988

Contents lists available at ScienceDirect

Chemical Engineering Journal

journal homepage: www.elsevier.com/locate/cej

Effect of LiCl concentration in the polymer dope on the structure and performance of hydrophobic PVDF hollow fiber membranes for CO_2 absorption

A. Mansourizadeh [a,b], A.F. Ismail [a,c,*]

[a] Advanced Membrane Technology Research Centre (AMTEC), Universiti Teknologi Malaysia, 81310 Skudai, Johor, Malaysia
[b] Department of Gas Engineering, Faculty of Petroleum and Renewable Energy Engineering (FPREE), Universiti Teknologi Malaysia, 81310 Skudai, Johor., Malaysia
[c] Materials and Manufacturing Research Alliance (MMRA), Universiti Teknologi Malaysia, 81310 Skudai, Johor, Malaysia

ARTICLE INFO

Article history:
Received 23 March 2010
Received in revised form
29 September 2010
Accepted 14 October 2010

Keywords:
PVDF hollow fiber membrane
Non-solvent additive
Characterization
CO_2 absorption
Membrane contactor

ABSTRACT

Effect of lithium chloride (LiCl) concentration as non-solvent additive in the spinning dopes on the structure and CO_2 absorption performance of the polyvinylidene fluoride (PVDF) membranes was investigated. The hollow fiber membranes were prepared via a wet phase-inversion process and characterized in terms of gas permeability, wetting resistance, mass transfer resistance and overall porosity. The morphology study indicated that by increasing LiCl concentration in the spinning dope, the membrane structure changed from the finger-like to the sponge-like. In addition, by increasing LiCl concentration up to 4 wt.% a drastic decrease in the N_2 permeance and a significant increase in the wetting resistance were observed. CO_2 absorption by distilled water was conducted through the gas–liquid membrane contactors. Using LiCl in the spinning dopes, the CO_2 flux of the prepared membranes significantly improved. By introducing 2 wt.% LiCl, the PVDF membrane showed a CO_2 flux of approximately 60% higher than the plain PVDF membrane at the absorbent flow rate of 200 ml/min. It can be concluded that a porous hydrophobic hollow fiber membrane with improved structure can be a productive alternative for CO_2 absorption and separation through gas–liquid membrane contactors.

1. Introduction

One-third of CO_2 emission comes from combustion of fossil fuels in power plants worldwide, which has been associated with global climate change and acidic rains [1]. Besides, presence of CO_2 in natural gas can cause pipeline and equipment corrosion, reduction in the heating value and occupying the volume in the pipeline [2]. Hence, environmental, economical and operational effects are the main reasons for CO_2 removal from the gas streams. For this purpose, several techniques have been improved such as chemical and physical absorption, solid adsorption, cryogenic distillation and membrane separation [3].

Alkanolamine based gas absorption is the most common process for the acid gas treating in operation due to the flexibility and ability to remove the acid gas to very low levels [4]. Although, such devices have attained significant success in the industries, they suffer from some operational drawbacks such as foaming, flooding, channeling and entrainment. In addition, because of their relatively smaller mass transfer coefficient, they tend to be large and costly to build. Therefore, in order to minimize overall environmental impacts and cost of CO_2 capture, the priority will be given to the technologies with improved CO_2 removal efficiency.

Hollow fiber gas–liquid membrane contactor is a promising alternative to conventional gas absorption systems for CO_2 capture from the gas streams. In this system, membrane separation is not only combined with an absorption process, but both processes are fully integrated into one piece of equipment. The porous membrane acts as a fixed interface between the gas and liquid phases without dispersing one phase into another. The porous membrane offers a flexible modular device with a high specific surface area. The absorption process can offer a very high selectivity and a high driving force for transport even at very low concentrations [5].

The first membrane gas absorption process for CO_2 removal from the gas stream was conducted by Qi and Cussler [6,7], which has led to a number of studies on the improvement of CO_2 capture by gas–liquid membrane contactors [8–15]. The membrane is the most important element of the membrane gas absorption process that requires essential properties such as high hydrophobicity, high surface porosity, low mass transfer resistance and excellent resistance to various chemical-feed streams. In order to minimize the membrane mass transfer resistance, not only the membrane should possess high permeability but also the pores of membrane must be completely gas-filled over the prolonged periods of operational time. This can be achieved by using hydrophobic membrane with small pore size.

* Corresponding author. Tel.: +60 7 5535 592; fax: +60 7 5581 463.
E-mail address: afauzi@utm.my (A.F. Ismail).

1385-8947/$ – see front matter © 2010 Elsevier B.V. All rights reserved.
doi:10.1016/j.cej.2010.10.034

Polypropylene (PP), polyethylene (PE), polytetrafluorethylene (PTFE) and poly (vinylidene fluoride) (PVDF) are the most popular hydrophobic polymeric materials. However, PE, PP and PTFE cannot be dissolved in the common solvents at low temperature. Hence, these membranes are usually prepared by stretching and thermal methods which result in a symmetric structure with relatively large pore sizes. PVDF is the only hydrophobic polymer soluble in the organic solvents, which can be used in the phase-inversion process for asymmetric membrane preparation. However, it should be noted that the formation of membranes using semi-crystalline polymers such as PVDF is relatively difficult compared to glassy polymers, since it is controlled by liquid–liquid demixing and crystallization in phase-inversion process [16]. In fact, liquid–liquid demixing results in open cellular structure which is common for glassy polymers, meanwhile crystallization process provides microporous structure with interlinked crystalline particles [17]. Consequently, the combination of both processes result in the final membrane structure.

In addition, by introducing a non-solvent additive in the polymer dope, the phase-inversion process can be modified to produce porous membrane structure. It was found that the addition of polyvinylpyrrolidone (PVP) in the PVDF dope resulted in the membranes with a slight decrease in the mean pore size and a drastic increase in the effective porosity as compared to that without addition of PVP [18]. Since the PVP has a high molecular weight, it cannot completely wash out from the membrane structure during solvent/non-solvent exchange and later washing process. A trace of PVP in the membrane can seriously affect the membrane hydrophobicity. Yeow et al. [19] have studied effects of different additives such as water, glycerol, lithium per-chlorate and ethanol on the PVDF membrane morphology. Their results indicated that the membrane permeation flux increased as more water was added in the polymer dope. Moreover, it was found that glycerol and phosphoric acid as an additive in the PVDF polymer dope showed a larger pore size and a higher value of molecular weight cut off (MWCO) compared to water, which improved the membrane permeability and CO_2 absorption flux [11]. This indicates that using non-solvent additives with small molecular weight and high water soluble properties, which can be easily washed out during membrane preparation, is preferred for preparing PVDF membranes with high permeability and good hydrophobicity.

Lithium chloride (LiCl) has been used as pore forming agent to prepare porous PVDF membranes for different applications. However, its effect on the phase-inversion process and the prepared membrane structure for CO_2 absorption is scarcely reported in the open literature. It was found by Wang et al. [20] that the prepared asymmetric porous PVDF hollow fiber membranes demonstrated high gas permeability, good mechanical strength and excellent hydrophobicity, once water/LiCl or 1-propanol/LiCl used as the additives in the spinning dopes. LiCl at high concentration (7.5%) in the PVDF homopolymer solution resulted in suppressing macrovoid formation, however at low concentration (2.5%), it enhanced permeate flux [21]. The high performance PVDF hollow fiber membranes were also prepared for desalination of water through direct contact membrane distillation, when LiCl and polyethylene glycol 1500 were introduced in the polymer dope [22]. During the desalination process of 3.5 wt.% sodium chloride solution, the rejection of NaCl maintained 99.99% with the feed solution at 81.8 °C for about 200 h continuous operation.

In our previous study, it was found that the addition of strong non-solvent such as glycerol in the polysulfone (PSF) and PVDF spinning dopes resulted in the membrane structure with enhanced CO_2 flux [23]. In the present study, different concentration of LiCl in the PVDF spinning dopes was considered to prepare asymmetric PVDF hollow fiber membranes via a wet phase-inversion process.

Table 1
Spinning dopes composition and viscosity.

Spinning dope	D1	D2	D3
PVDF (wt.%)	18	18	18
LiCl (wt.%)	0	2	4
NMP (wt.%)	82	80	78
Viscosity (cp at 25 °C)	2815	5536	13,130

The main purpose of the study was to improve the membrane structure for CO_2 absorption. The prepared hollow fiber membranes were characterized in terms of gas permeability, mass transfer resistance and wetting resistance, which are the most important membrane parameters for gas absorption applications. The performance of the membranes for CO_2 absorption was examined through the gas–liquid membrane contactors.

2. Experimental

2.1. Materials

Commercial PVDF polymer pellets (Kynar® 740, Mn = 156,000) were supplied by Arkema Inc., Philadelphia, USA. 1-Methyl-2-pyrrolidone (NMP, >99.5%) was used as polymer solvent without further purification. Lithium chloride (LiCl, ≥99%) (Sigma–Aldrich®) was used as non-solvent additives in the polymer dopes. Methanol (GR grade, 99.9%) and n-hexane (99%) were purchased from MERCK and used as post-treating the prepared membranes. Tap water was used as coagulation bath in the spinning process. Distilled water was used as liquid absorbent in the CO_2 absorption experiments.

2.2. Fabrication of porous hollow fiber membranes

The PVDF polymer pellets were dried at 60 ± 2°C in a vacuum oven for 24 h to remove moisture content. The spinning dopes were prepared at 60 °C using stirring until the solution became homogeneous. In order to remove suspended gas-bubbles from the solutions, ultrasonic degassing was applied for 30 min and the solutions were kept for 24 h at room temperature before spinning. The resulting solutions composition and viscosity are given in Table 1. The hollow fiber spinning apparatus by the dry-jet wet phase-inversion was explained elsewhere [24]. Table 2 lists the detailed spinning parameters.

The spun fibers were immersed in water for 3 days to remove the residual NMP and the additive. Then they were post-treated using methanol and n-hexane as non-solvent exchange to minimize fiber shrinkage and pores collapse before drying at room temperature.

2.3. Field emission scanning electron microscopy (FESEM) examination

Field emission scanning electronic microscopy (FESEM) (ZEIZZ SUPRA 35VP) was used to examine the morphology of the spun PVDF hollow fiber membranes by the standard methods. The membrane samples were immersed in liquid nitrogen and fractured

Table 2
Hollow fiber spinning conditions.

Dope extrusion rate (ml/min)	4.5
Bore flow rate (ml/min)	1.55
Bore composition (wt.%)	NMP/H_2O 80/20
External coagulant	Tap water
Air gap distance (cm)	0.50
Spinneret o.d./i.d. (mm)	1.2/0.55
Spinning dope temperature (°C)	25
External coagulant temperature (°C)	25

carefully. Then the samples were dried in a vacuum oven and coated by sputtering platinum before testing. The FESEM micrographs of cross-section, internal surface, external surface and outer skin layer of the hollow fibers were taken at various magnifications.

2.4. Gas permeation test

A gas permeation method was applied to determine the mean pore size and the effective surface porosity over the effective pore length of the asymmetric membrane. For a significant porous membrane, the total gas permeation rate through the membrane can be considered as the combination of Poiseuille flow and Knudsen flow [25].

By assuming cylindrical pores in the skin layer of the asymmetric membranes, the gas permeance can be calculated [8]:

$$J_A = \frac{2r_p\varepsilon}{3RTL_p}\left(\frac{8RT}{\pi M}\right)^{0.5} + \frac{r_p^2\varepsilon}{8\mu RTL_p}\bar{P} \quad \text{or} \quad J_A = K_0 + P_0\bar{P} \tag{1}$$

where J_A is the gas permeance (mol/m^2 s Pa); r_p and L_p are pore radius and effective pore length, respectively (m); ε is surface porosity; R is gas constant 8.314 (J/mol K); μ is gas viscosity (kg/m s); M is gas molecular weight; T is gas temperature (K); and $\bar{P}$ is mean pressure (Pa).

By plotting J_A with mean pressures according to Eq. (1), mean pore size and effective surface porosity over pore length, ε/L_p, can be calculated from the intercept (K_0) and slope (P_0) as following:

$$r_p = 5.333\left(\frac{P_0}{K_0}\right)\left(\frac{8RT}{\pi M}\right)^{0.5}\mu \tag{2}$$

$$\frac{\varepsilon}{L_p} = \frac{8\mu RTP_0}{r_p^2} \tag{3}$$

In the gas permeation method, pure N_2 was used as the test gas. The test apparatus used was based on the volume displacement method [26]. The test module containing two hollow fibers with the length of about 10 cm was used to determine the gas permeability. The upstream pressure was increased at 0.25×10^5 Pa intervals up to 2×10^5 Pa. The N_2 permeation rate was measured at 25 °C in the lumen side using soap-bubble flow meter. The gas permeability was then calculated according to outer diameter of the hollow fiber.

2.5. Critical water entry pressure, collapsing pressure and overall porosity measurement

Critical water entry pressure (CEP_w) test was applied to characterize the prepared membranes in terms of wetting resistance. Based on the Laplace–Young equation, for a given membrane structure, wetting resistance of the membrane is related to the surface hydrophobicity and membrane pore sizes [27]. The minimum liquid pressure required to penetrate in the membrane pores can be estimated by:

$$\Delta P = -\frac{2\gamma\cos\theta}{r_{p,max}} \tag{4}$$

where γ is surface tension of the liquid (N/m); θ is the contact angle between the membrane surface and liquid; and $r_{p,max}$ is the maximum pore size of the membrane (m).

In order to measure the wetting resistance, distilled water was fed into the lumen side of the hollow fiber membranes using a diaphragm pump. The pressure slowly increased at 0.5×10^5 Pa interval. At each pressure interval, the membrane module was kept at the constant pressure for 30 min to check if any water droplet appeared in the outer surface of the fiber. CEP_w was considered as the pressure for the first water droplet in the outer surface of the hollow fiber.

Table 3
Characteristics of the gas–liquid membrane contactor.

Module i.d. (mm)	14
Module length (mm)	270
Fiber o.d. (mm)	0.75
Fiber i.d. (mm)	0.42
Effective fiber length (mm)	150
Number of fibers	10
Surface area (m^2/m^3)	153

Mechanical stability of the hollow fiber membranes was examined through collapsing pressure measurements. During the gas permeation test, the upstream pressure in the shell side of the membrane module was further increased at 0.25×10^5 Pa intervals. At each pressure interval, the membrane module was kept at the constant pressure for 5 min. Collapsing pressure was considered as the pressure where a sudden decrease in the permeate flow in lumen side appeared.

For the determination of the overall porosity, five hollow fibers with the length of 50 cm were dried for 2 h at 105 °C in a vacuum oven and weighed. The overall porosity was calculated according to the commonly used method based on density measurements [28]:

$$\varepsilon\ (\%) = \left(1 - \frac{\rho_f}{\rho_p}\right) \times 100 \tag{5}$$

where ρ_f and ρ_p are the fiber and polymer density, respectively. The fiber density was calculated from the mass and volume ratio as:

$$\rho_f = \frac{4w}{\pi(d_o^2 - d_i^2)L} \tag{6}$$

where L is the fiber length; w is fiber mass; d_i and d_o are the inner and the outer diameter, respectively. The density of the PVDF polymer is 1.77 g/cm^3.

2.6. CO_2 absorption experiment

The gas–liquid membrane contactor was employed to determine the membrane mass transfer resistance and CO_2 absorption flux of the membranes, where a total of 10 hollow fibers were packed randomly in the stainless steel module. Table 3 shows the specifics of the membrane contactor module. Pure CO_2 as the feed gas and distilled water as the liquid absorbent were used in the membrane contactor to measure absorption flux. A counter-current flow was used for the gas and the liquid absorbent. A continuous mode of operation was conducted at 1×10^5 Pa CO_2 pressure and 25 °C temperature. The liquid absorbent pressure was controlled 0.2×10^5 higher than CO_2 pressure in order to prevent bubble formation in the liquid phase. Using the chemical titration method, CO_2 concentration in the liquid outflow at various flow rates was measured to determine the CO_2 flux. Before taking the samples, all the experiments were carried out for 30 min to achieve a steady state condition. The flow diagram of the experimental setup is given in Fig. 1.

2.6.1. Measurement of the membranes mass transfer resistance

The membranes mass transfer resistance can be obtained using the Wilson plot method [29], quantitatively. Generally, for a hydrophobic hollow fiber membrane with gas filled pores, the overall mass transfer resistance (K_o^{-1}) can be expressed by a resistance in the series model [30,31]:

$$\frac{1}{K_o} = \frac{m}{k_g d_o/d_i} + \frac{m}{k_m d_{lm}/d_i} + \frac{1}{Ek_l} \tag{7}$$

where k_g is the gas side mass transfer coefficient (m/s); k_m is the membrane mass transfer coefficient (m/s); k_l is the liquid phase

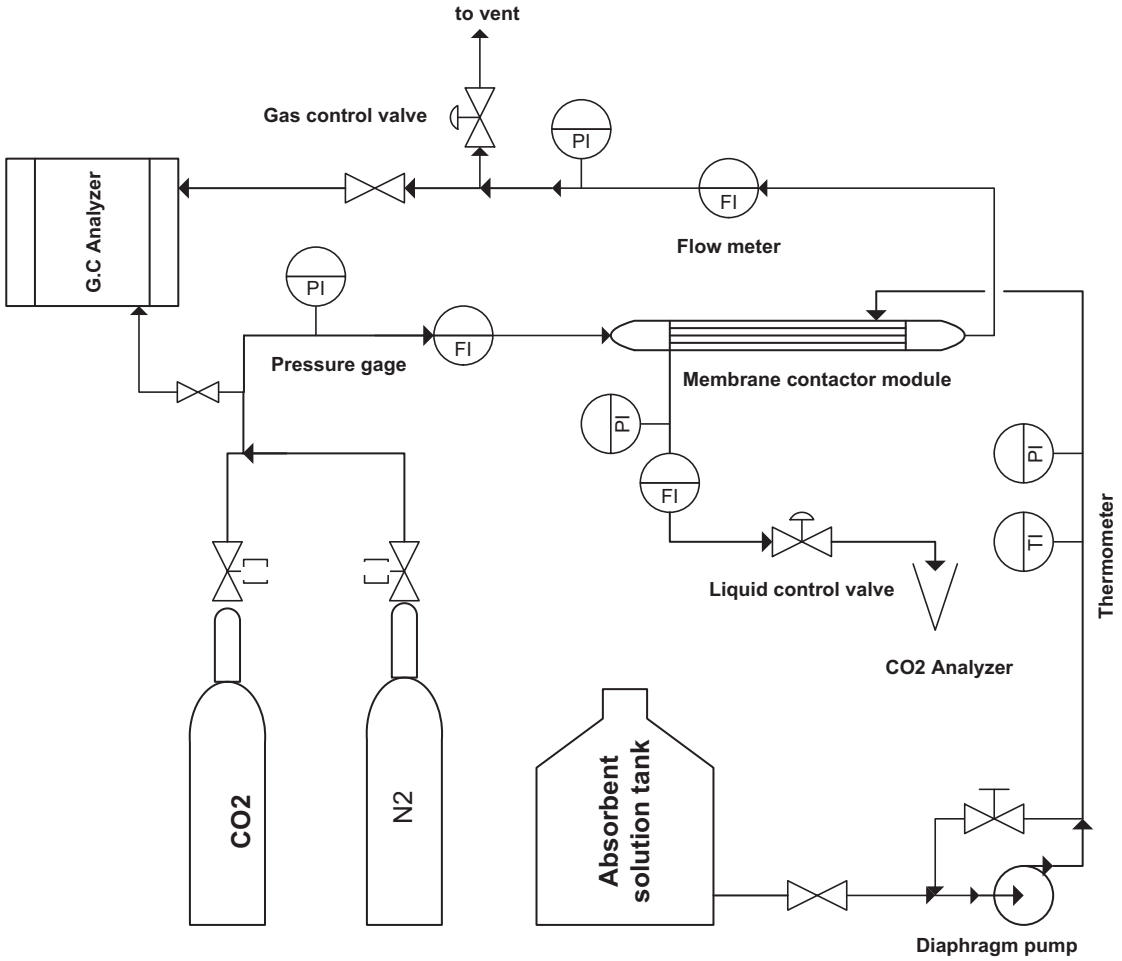

Fig. 1. Flow diagram of experimental setup for CO_2 absorption.

mass transfer coefficient (m/s); d_o is the outer diameter of hollow fiber membrane (m); d_i is the inner diameter of hollow fiber membrane (m); d_{lm} is the log mean diameter (m); m is the distribution coefficient between gas and liquid phase which can be replaced by Henry's law constant (H); and E is the enhancement factor due to chemical reaction.

In case of physical absorption with water the gas side mass transfer resistance can be ignored because pure CO_2 was used as the feed gas. Therefore, it can be assumed that only the liquid and the membrane mass transfer resistances are contributed to the mass transfer process. The liquid mass transfer resistance is proportional to the liquid velocity $U_l^{-\alpha}$, where α is an empirical constant and U_l is liquid velocity. A plot of K_o^{-1} versus $U_l^{-\alpha}$ results in a straight line, which is known as Wilson plot. The value of α is selected as the one that provides the best straight line through the data points. The membrane mass transfer resistance is given by the intercept of the Wilson plot. The overall mass transfer coefficient was determined by mass balance across the length of hollow fibers [14]:

$$K_o = -\frac{Q_l}{A_i} \ln\left(1 - \frac{C_{l,o}}{HC_g}\right) \quad (8)$$

where Q_l is liquid flow rate (m^3/s), A_i is inner surface of hollow fibers or gas–liquid contact area (m^2); $C_{l,o}$ and C_g are liquid outlet and gas side concentration respectively (mol/m^3); and H is Henry's law constant, which is 0.85 for CO_2–water system [32].

3. Results and discussion

3.1. Morphology of the PVDF hollow fiber membranes

In general, by controlling the phase-inversion rate and rheology of the spinning dope, the membrane structure can be modified for particular applications. It was proven that more porous asymmetric membranes can be fabricated by increasing phase-inversion rate of the polymer solution [20,33]. In addition, formation of macrovoids in the membrane structure is significantly affected by shear rate of the solution through the spinneret [34]. In order to prepare porous membranes with improved structure for CO_2 absorption, different amounts of LiCl were introduced into the spinning dopes as a phase-inversion promoter additive. The morphology of the prepared PVDF membranes was examined through FESEM. The cross-sectional structure of the membranes is presented in Fig. 2. The hollow fiber membranes possess outer diameters ranging from 700 to 770 μm, inner diameters ranging from 415 to 470 μm and the wall thickness ranging from 110 to 135 μm. Since all the fibers were spun at the same dope extrusion rate and spinning conditions, almost a similar dimension was obtained for the hollow fiber membranes. For cross-section morphology, the membrane structure changed from finger-like to sponge-like by increasing the amount of LiCl in the spinning dopes. The prepared PVDF membranes without LiCl showed an almost finger-like structure, where the finger-likes enlarged close to the inner surface (up to 105 μm). On the other hand, addition of 4 wt.% LiCl in the spinning dope provided a sponge-like structure with very small finger-likes (up to

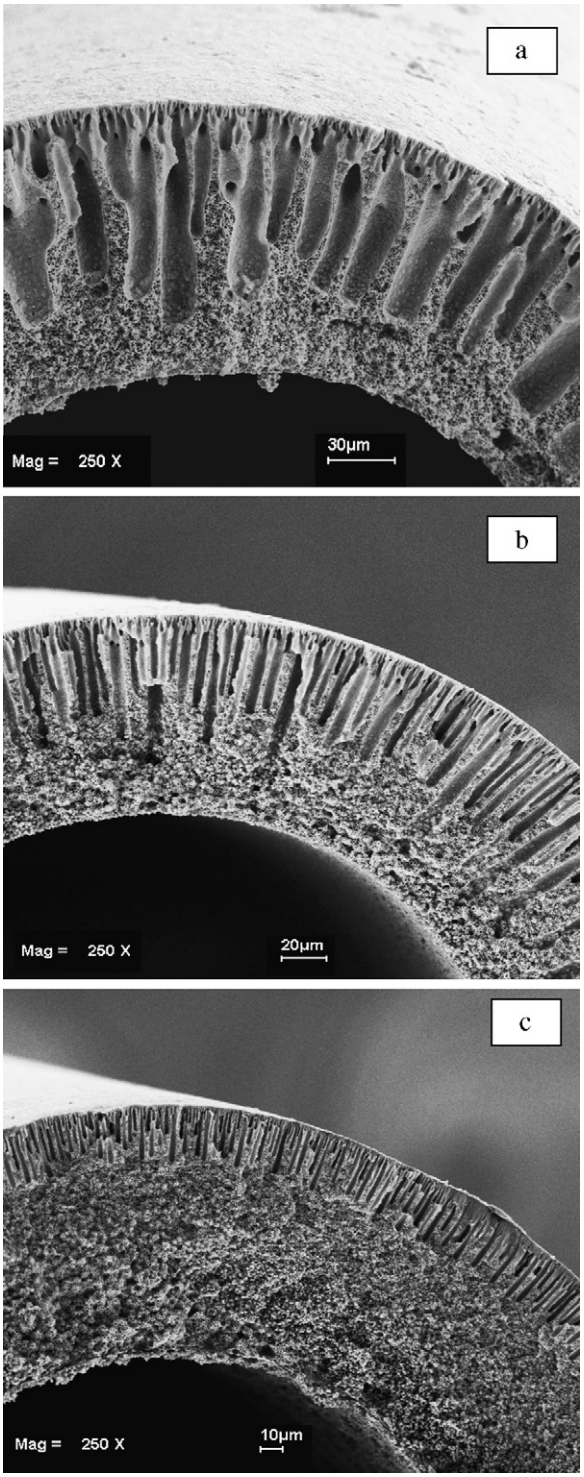

Fig. 2. Cross-sectional morphology of the PVDF hollow fiber membranes: (a) plain PVDF; (b) 2 wt.% LiCl; and (c) 4 wt.% LiCl.

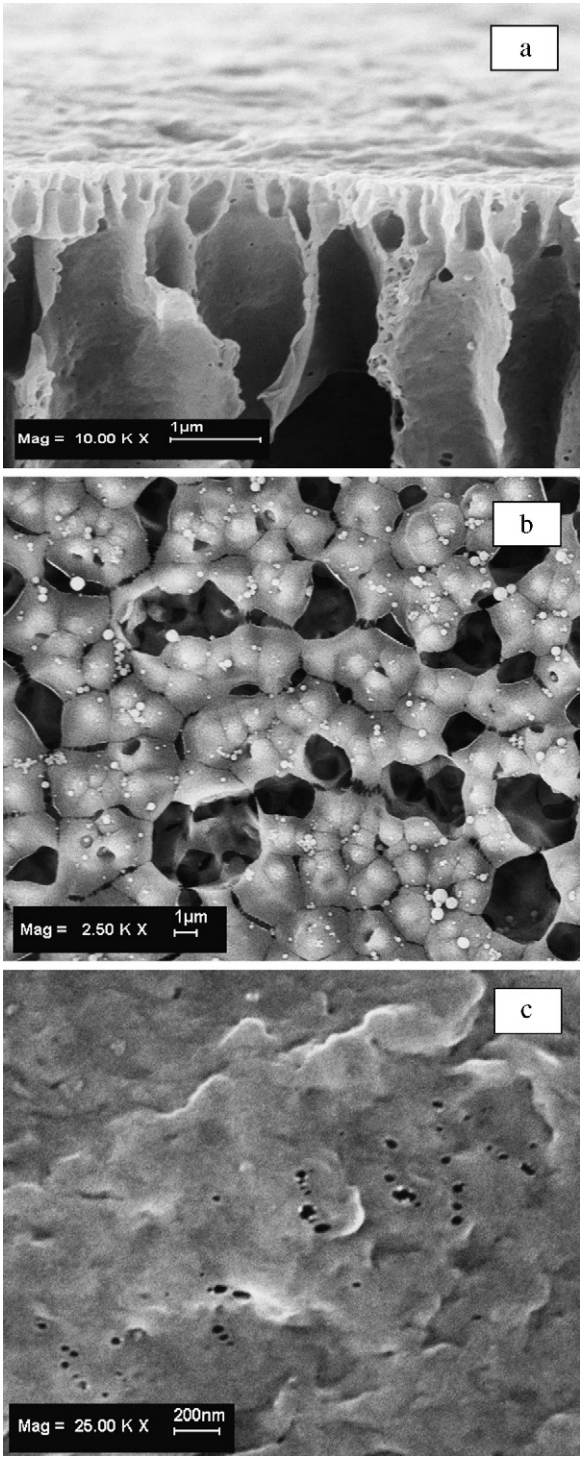

Fig. 3. FESEM micrographs of the PVDF hollow fiber membranes (2 wt.% LiCl in the polymer dope): (a) skin layer; (b) inner surface; and (c) outer surface.

30 μm) beneath the outer surface. This phenomenon can be related to the spinning dopes viscosity and consequent increase of shear stress in the spinneret. From Table 1, by increasing the LiCl concentration, viscosity of the spinning dopes drastically increased. In fact, the significant increase in the spinning dope containing LiCl can be associated to the formation of a complex between organic solvents and LiCl and/or macromolecular changeable networks between LiCl and an electron donor group of PVDF [35]. Generally, addition of non-solvent additives in the polymer dopes results in enhancement of liquid–liquid demixing, which provides membranes with finger-like structure. Meanwhile, the additives can also increase the polymer dopes viscosity, which generates membranes with sponge-like structure [10,11]. In fact, an increase in the viscosity of the spinning dope can result in a decrease in mutual diffusion between solvent in the spinning dope and non-solvent (water) in the coagulation bath. In addition, it was also proven that an increase in the shear stress could suppress the formation of finger-like macrovoids [34]. Therefore, it can be said that both effects control the sponge-like structure of the membrane.

Table 4
Characteristics of the PVDF hollow fiber membranes.

Membrane	N_2 permeance at 1×10^5 Pa (10^{-3} cm^3/cm^2 s cmHg)	Mean pore size (nm)	Effective surface porosity ε/L_p ($\times 10^2$ m^{-1})	CEP_w ($\times 10^5$ Pa)	Collapsing pressure ($\times 10^5$ Pa)	Overall porosity (%)
PVDF	22.50	7.18	4210	1.00	7.50	72.01
PVDF + 2% LiCl	20.30	3.80	7540	2.00	7.50	67.26
PVDF + 4% LiCl	6.69	3.96	2410	6.50	8.25	65.63

Furthermore, 2 wt.% LiCl in the spinning dope resulted in further enlargement of the finger-likes (up to 60 μm), which provided an almost finger-like/sponge-like structure. This structure expected to provide higher permeability (lower mass transfer resistance) favorable for gas absorption application.

Fig. 3 shows that the skin layer, inner surface and outer surface morphology of the PVDF membrane prepared by 2 wt.% LiCl in the spinning dope, are almost the same for all the prepared membranes. All the membranes showed an ultra thin skin layer. From FESEM examination, the skin layer thickness of the membranes slightly increased by increasing the spinning dope viscosity. By increasing LiCl concentration from 2% to 4%, the skin layer thickness increased from 65 to 100 nm. The higher shear stress in the spinneret due to the increase of viscosity resulted in the thicker skin layer. Indeed, molecular chains of the polymer tend to align themselves much better at higher shear. This greater molecular orientation results in closer packing of the polymer molecules and denser outer skin layer [36]. Eventually, a lower surface porosity is expected for the membranes with denser outer skin layer, which is confirmed by the results of gas permeation test.

As for the inner surface formation, using 80 wt.% NMP solution as the bore fluid induced delay phase-inversion and provided an inner skinless surface with open microporous structure (Fig. 3b). Due to the high solvent concentration in the bore side, the polymer concentration at this region was prevented and solidification of the localized polymer-rich phase produced an interconnected open-cell structure. The same morphology was also obtained for the polysulfone membranes using 95 wt.% NMP as the bore fluid [15]. In fact, removing the inner skin layer can minimize the membrane mass transfer resistance during gas absorption process [13].

3.2. Characterization of the hollow fiber membranes

Different LiCl concentrations were considered in the spinning dopes in order to prepare the asymmetric membranes with high permeability (low mass transfer resistance) and hydrophobicity (high wetting resistance). The hollow fiber membranes were characterized in terms of gas permeability, critical water entry pressure and overall porosity. The results are given in Table 4.

In general, overall porosity of the asymmetric membranes can be governed by the polymer dope composition. From Table 4, all the membranes possess a good overall porosity, which can be a result of the low polymer concentration (18 wt.%) in the spinning dopes. Moreover, by increasing LiCl concentration in the spinning dopes the overall porosity slightly decreased due to the change in the membrane morphology from finger-like to sponge-like structure. Since, the fiber overall porosity is measured on the basis of the void fraction, it seems that the finger-like structure provides higher void fractions compared to sponge-like structure membranes.

Collapsing pressure test was conducted to estimate mechanical stability of the hollow fiber membranes. As shown in Table 4, the sponge-like structure of the PVDF membrane prepared by 4% LiCl showed slightly higher collapsing pressure. The addition of LiCl could significantly reduce macrovoids in the membrane structure and resulted in higher mechanical stability. Similar results were reported that the addition of PVP in the polymer dope could suppress the macrovoids formation and improved the mechanical strength of the hollow fibers [37]. It is worth mentioning that a minimum pressure difference between the gas and liquid phases is required to perform membrane gas absorption [14], however, higher mechanical stability of the membrane is more appropriate for unsteady operating conditions.

Critical water entry pressure (CEP_w) test was conducted to examine wetting resistance of the prepared membranes. Indeed, long-term stable operation of the gas–liquid membrane contactor requires that the pores of membrane remain completely gas-filled. Therefore, using hydrophobic membranes with a high wetting resistance are desired for long-term gas absorption applications. From Table 4, the CEP_w of the membranes considerably increased by increasing LiCl concentration in the spinning dopes, which can be associated to the membranes structure. In fact, the finger-likes provide an open membrane structure with low degree of tortuosity through which water can easily pass through the membrane pores and wet the membrane. However, the sponge-like structure can withstand wetting during gas absorption process as the PVDF membrane prepared by 4 wt.% LiCl indicated significantly high CEP_w.

Fig. 4 shows N_2 permeance of the membranes as a function of mean pressure. The solid lines indicate the best linear fit to the data. Based on Eq. (1) given in the preceding section, the values of P_0 and K_0 can be obtained from intercept and slope of the lines in Fig. 4, respectively. Both the values of P_0 and K_0 can then be employed to calculate the mean pore size and the effective surface porosity using Eqs. (2) and (3). The results are given in Table 4. From Fig. 4, the slope of N_2 permeance line for the plain PVDF membranes is rationally higher than the prepared membranes by using LiCl in the spinning dopes. It means that both the Poiseuille and Knudsen flows govern the N_2 permeation through the membrane. On the other hand, the slope of lines for the prepared membranes using 2 and 4 wt.% LiCl is significantly low. It seems that the Knudsen flow governs the N_2 permeation through the membranes, which can confirm existence of small pore sizes (see Table 4). Moreover, addition of LiCl in the spinning dopes significantly decreased the intercept of the lines, which indicates lower permeability of the membranes. This can be related to the sponge-like morphology of

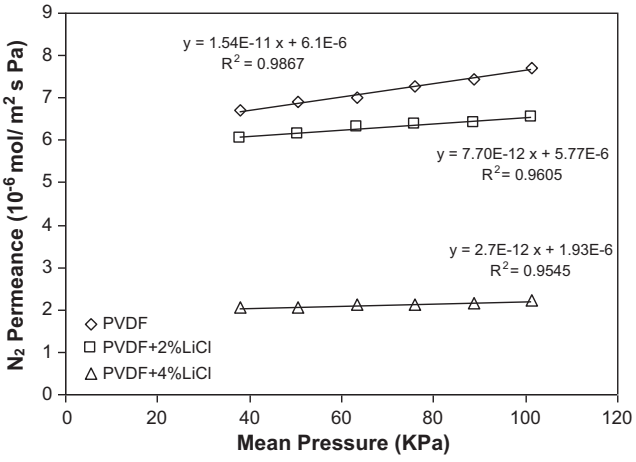

Fig. 4. Measured N_2 permeance of the PVDF hollow fiber membranes.

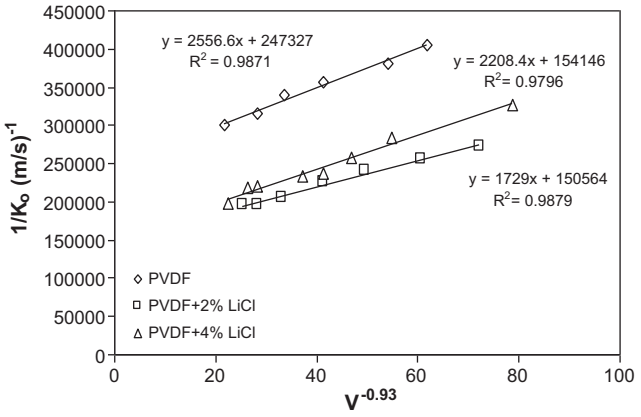

Fig. 5. Wilson plot of the PVDF hollow fiber membranes (pure CO_2-distilled water system).

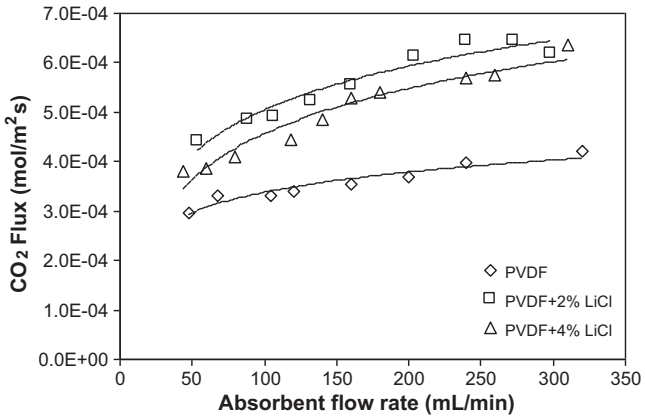

Fig. 6. CO_2 absorption performance of the PVDF hollow fiber membranes (pure CO_2-distilled water system).

the membrane, which gives the denser structure with higher degree of tortuosity.

To determine the membranes mass transfer resistance, the Wilson plots of $1/K_o$ versus $V^{-0.93}$ were obtained as shown in Fig. 5. The α value of 0.93 was found to represent the best linear fit to the data of Wilson plot. A similar relationship of $1/K_o$ with $V^{-0.93}$ was correlated by Yang and Cussler [38] to describe the gas absorption in the shell side of the membrane module. As discussed earlier, by considering resistances in series model, the intercept of the plots give the membranes mass transfer resistance. Using 2 wt.% LiCl in the spinning dope resulted in the membrane structure with the lowest mass transfer resistance. Since 2 wt.% LiCl in the spinning dope provided finger-like/sponge-like structure with high permeability and reasonable wetting resistance the lowest mass transfer resistance was obtained. Meanwhile, the membranes prepared by 4 wt.% LiCl possess high wetting resistance and relatively low permeability which indicated higher mass transfer resistance. It can be concluded that wetting resistance and gas permeability are two important parameters which can affect the membrane mass transfer resistance. Therefore, an improved membrane structure for gas absorption application can be achieved by the trade off between these two parameters.

3.3. CO_2 absorption performance of the membranes

In our previous studies, different porous hollow fiber membranes were prepared for CO_2 absorption according to the aspects of phase-inversion process [12,15,23]. Using desire amount of strong non-solvent additives such as glycerol, ortho-phosphoric acid (PA) and lithium chloride monohydrate ($LiCl{\cdot}H_2O$) in the polymer solutions resulted in the membranes with enhanced CO_2 flux. It was found that hydrophobicity, permeability and wetting resistance of the membrane are important factors for gas absorption applications, which mainly depend on the membrane structure. Introducing glycerol in the PSF spinning dope resulted in the membrane with improved CO_2 flux compared to plain PSF membrane. However, its lower hydrophobicity and permeability compared to PVDF membranes can cause unviable long-term operation. The PVDF hollow fiber membranes were prepared by using the amount of PA and $LiCl{\cdot}H_2O$ close to cloud point values of the polymer solution. Although the membranes demonstrated good wetting resistance, almost fully sponge-like structure of the membranes with low permeability (surface porosity) limited CO_2 absorption improvement. In the present study, an attempt was made to achieve improved membrane structure for CO_2 absorption by adjusting the amount of a strong non-solvent additive like LiCl in the PVDF solutions.

Physical CO_2 absorption with distilled water was conducted in the gas–liquid membrane contactor at 25 °C. The liquid absorbent passed through the shell side in contact with skin layer of the membranes and pure CO_2 flowed counter-currently through the lumen side of the hollow fiber membranes. The CO_2 absorption performance of the prepared PVDF membranes was compared and the results are given in Fig. 6. It was observed that the CO_2 flux of all the membranes increased with an increase in the absorbents flow rate. This can be associated to the decrease of liquid boundary layer thickness around the fibers with increasing liquid velocity, which led to a reduction in the liquid mass transfer resistance and CO_2 saturation.

From Fig. 6, with addition of LiCl in the spinning dopes, the CO_2 absorption flux of the membranes significantly improved. Moreover, the CO_2 absorption rate of the PVDF/LiCl membranes increased relatively faster than the plain PVDF membrane with a greater increase in the absorbent flow rate. By increasing the absorbent flow rate from 50 to 200 ml/min, the CO_2 flux of the PVDF membrane with 2 wt.% LiCl increased from 4.40×10^{-4} to 6.12×10^{-4} mol/m^2 s. This shows an approximate 40% improvement in the CO_2 flux; meanwhile the plain PVDF membrane demonstrates 23% improvement in the flux. It can be said that the performance of the membranes is mainly related to the membrane structure. Since the plain PVDF membrane has finger-like structure with larger pore sizes the value of CEP_w is significantly low. Hence, the membrane can easily be wetted during initial stages of absorption process. The slow increase in the CO_2 flux with the absorbent flow rate can confirm gradual wetting of the membrane, where the membrane resistance controls the mass transfer process. It was proven that partial wetting could increase the overall mass transfer resistance rapidly and thus significantly affected the absorption flux during the operation [10].

Addition of 2 wt.% LiCl in the spinning dope resulted in the PVDF hollow fiber membrane structure with considerably improved CO_2 flux. At 200 ml/min of the absorbent flow rate, CO_2 flux of 6.14×10^{-4} mol/m^2 s was observed, which indicated an approximate 60% higher CO_2 flux than the plain PVDF membrane. As discussed earlier, the membrane has finger-like/sponge-like structure with small pore sizes and higher surface porosity. Indeed, higher surface porosity provides higher contact area between gas and liquid phases in the membrane contactor and the small pore sizes resist wetting that can improve the absorption performance. It should be noted that the finger-like structure results in high permeability and low wetting resistance; meanwhile the sponge-like structure provides low permeability and high wetting resistance [12]. Therefore, a trade off between these two parameters can give an optimum membrane structure. The results demonstrated that

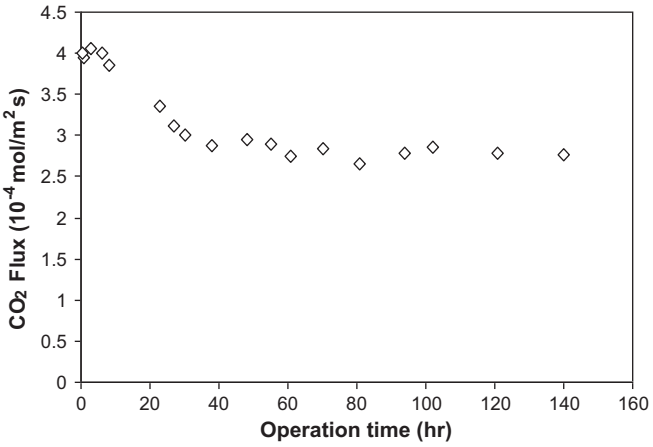

Fig. 7. Long-term CO_2 absorption performance of the PVDF + 4% LiCl membrane (Q_l = 80 ml/min, Q_g = 100 ml/min, $P_g = P_l = 1 \times 10^5$ Pa).

the finger-like/sponge-like structure of the PVDF membrane prepared by 2 wt.% LiCl enhanced the CO_2 absorption performance.

Although the membrane prepared by 4 wt.% LiCl in the spinning dope showed slightly lower CO_2 flux, it seems that its sponge-like structure with high CEP_w can resist wetting during the long-term operation. The CO_2 absorption performance of the membrane was examined for over 140 h and the results are given in Fig. 7. As it can be seen, the performance deterioration was started at initial short period of the operation and reached to a stable condition after around 25 h. Then the CO_2 absorption flux almost maintained stable until the end of the operation. The approximate 30% CO_2 flux reduction can be related to partial wetting of the membrane pores. Similar performance deterioration was observed for polypropylene hollow fiber membrane contactor for CO_2 absorption by water [39]. Although the membrane has very small pore sizes with high wetting resistance, partial wetting can be attributed to capillary condensation of water vapor in the membrane pores. In fact, the smaller pore sizes are more capable for capillary condensation based on the Kelvin equation, which indicates that even undersaturated vapors can be condensed in the very small channels [40].

4. Conclusion

In order to improve the membrane structure for CO_2 absorption, porous hydrophobic PVDF hollow fiber membranes were prepared via a simple wet phase-inversion process. LiCl was introduced into the spinning dope as phase-inversion promoter and 80% NMP solution was used as the bore fluid. The effect of LiCl concentration on the membrane structure and CO_2 absorption performance was investigated. Results showed that by increasing LiCl concentration in the spinning dopes the membrane structure changed from finger-like to sponge-like. Addition of 2 wt.% LiCl in the spinning dope provided the membrane with finger-like/sponge-like structure which significantly improved the CO_2 flux. At 200 ml/min of the absorbent flow rate, CO_2 flux of 6.14×10^{-4} mol/m^2 s was achieved, which was approximately 60% higher than the CO_2 flux of the plain PVDF hollow fiber membrane. Results of long-term performance of the PVDF + 4%LiCl membrane demonstrated an approximate 30% CO_2 flux reduction at initial short period, then the operation maintained stable for over 140 h. Therefore, it can be concluded that an improved asymmetric PVDF hollow fiber membrane structure can be achieved via phase-inversion process for CO_2 absorption and separation.

Acknowledgement

The authors gratefully acknowledge the financial support from the Ministry of Science, Technology and Environment, Malaysia, with the Grant number of 03-01-06-SF0282.

References

[1] H. Herzog, B. Eliasson, O. Kaarstad, Capturing greenhouse gases, Sci. Am. 182 (2000) 72–79.
[2] S. Atchariyawut, R. Jiraratananon, R. Wang, Separation of CO_2 from CH_4 by using gas–liquid membrane contacting process, J. Membr. Sci. 304 (2007) 163–172.
[3] P. Riemer, Green gas mitigation technologies, an overview of the CO_2 capture, storage and future activities of the IEA Greenhouse Gas R&D Programme, Energy Convers. Manage. 37 (1996) 665–670.
[4] S. Paul, A.K. Ghoshal, B. Mandal, Removal of CO_2 by single and blended aqueous alkanolamine solvents in hollow-fiber membrane contactor: modeling and simulation, Ind. Eng. Chem. Res. 46 (2007) 2576–2588.
[5] R. Klaassen, P. Feron, A. Jansen, Membrane contactor applications, Desalination 224 (2008) 81–87.
[6] Z. Qi, E.L. Cussler, Microporous hollow fibers for gas absorption. I. Mass transfer in the liquid, J. Membr. Sci. 23 (1985) 321–332.
[7] Z. Qi, E.L. Cussler, Microporous hollow fibers for gas absorption. II. Mass transfer across the membrane, J. Membr. Sci. 23 (1985) 333–345.
[8] K. Li, J.F. Kong, D. Wang, W.K. Teo, Tailor-made asymmetric PVDF hollow fiber for soluble gas removal, AIChE J. 45 (1999) 1211–1219.
[9] J.A. Delgado, M.A. Uguina, J.L. Sotelo, V.I. Águeda, A. Sanz, Simulation of CO_2 absorption into aqueous DEA using a hollow fiber membrane contactor: evaluation of contactor performance, Chem. Eng. J. 152 (2009) 396–405.
[10] R. Wang, H.Y. Zhang, P.H.M. Feron, D.T. Liang, Influence of membrane wetting on CO_2 capture in microporous hollow fiber membrane contactors, Sep. Purif. Technol. 46 (2005) 33–40.
[11] S. Atchariyawut, C. Feng, R. Wang, R. Jiraratananon, D.T. Liang, Effect of membrane structure on mass-transfer in the membrane gas–liquid contacting process using microporous PVDF hollow fibers, J. Membr. Sci. 285 (2006) 272–281.
[12] A. Mansourizadeh, A.F. Ismail, M.S. Abdullah, B.C. Ng, Preparation of polyvinylidene fluoride hollow fiber membranes for CO_2 absorption using phase-inversion promoter additives, J. Membr. Sci. 355 (2010) 200–207.
[13] A. Xu, A. Yang, S. Young, D. deMontigny, P. Tontiwachwuthikul, Effect of internal coagulant on effectiveness of polyvinylidene fluoride membrane for carbon dioxide separation and absorption, J. Membr. Sci. 311 (2008) 153–158.
[14] A. Mansourizadeh, A.F. Ismail, T. Matsuura, Effect of operating conditions on the physical and chemical CO_2 absorption through the PVDF hollow fiber membrane contactor, J. Membr. Sci. 353 (2010) 192–200.
[15] A. Mansourizadeh, A.F. Ismail, Effect of additives on the structure and performance of polysulfone hollow fiber membranes for CO_2 absorption, J. Membr. Sci. 348 (2010) 260–267.
[16] P. Sukitpaneenit, T.S. Chung, Molecular elucidation of morphology and mechanical properties of PVDF hollow fiber membranes from aspects of phase inversion, crystallization and rheology, J. Membr. Sci. 340 (2009) 192–205.
[17] T.H. Young, D.J. Lin, J.J. Gau, W.Y. Chuang, L.P. Cheng, Morphology of crystalline Nylon-6,10 membranes prepared by the immersion-precipitation process: competition between crystallization and liquid–liquid phase separation, Polymer 40 (1999) 5011–5021.
[18] S.P. Deshmukh, K. Li, Effect of ethanol composition in water coagulation bath on morphology of PVDF hollow fiber membranes, J. Membr. Sci. 150 (1998) 75–85.
[19] M.L. Yeow, Y.T. Liu, K. Li, Morphological study of poly(vinylidene fluoride) asymmetric membranes: effects of the solvent, additive, and dope temperature, J. Appl. Polym. Sci. 92 (2004) 1782–1789.
[20] D. Wang, K. Li, W.K. Teo, Porous PVDF asymmetric hollow fiber membranes prepared with the use of small molecular additives, J. Membr. Sci. 178 (2000) 13–23.
[21] E. Fontananova, J.C. Jansen, A. Cristiano, E. Curcio, E. Drioli, Effect of additives in the casting solution on the formation of PVDF membranes, Desalination 192 (2006) 190–197.
[22] D. Hou, J. Wang, D. Qu, Z. Luan, X. Ren, Fabrication and characterization of hydrophobic PVDF hollow fiber membranes for desalination through direct contact membrane distillation, Sep. Purif. Technol. 69 (2009) 78–86.
[23] A.F. Ismail, A. Mansourizadeh, A comparative study on the structure and performance of porous polyvinylidene fluoride and polysulfone hollow fiber membranes for CO_2 absorption, J. Membr. Sci., doi:10.1016/j.memsci.2010.09.021.
[24] A.F. Ismail, I.R. Dunkinb, S.L. Gallivanb, S.J. Shilton, Production of super selective polysulfone hollow fiber membranes for gas separation, Polymer 40 (1999) 6499–6506.
[25] J.M.S. Henis, M.K. Tripodi, Composite hollow fiber membranes for gas separation: the resistance model approach, J. Membr. Sci. 8 (1981) 233–246.
[26] A.F. Ismail, S.N. Kumari, Potential effect of potting resin on the performance of hollow fibre membrane modules in a CO_2/CH_4 gas separation system, J. Membr. Sci. 236 (2004) 183–191.

[27] A.C.M. Franken, J.A.M. Nolten, M.H.V. Mulder, D. Bargeman, C.A. Smolders, Wetting criteria for the applicability of membrane distillation, J. Membr. Sci. 33 (1987) 315–328.
[28] J. Xu, Z.-L. Xu, Poly(vinyl chloride) (PVC) hollow fiber ultrafiltration membranes prepared from PVC/additives/solvent, J. Membr. Sci. 208 (2002) 203–212.
[29] E.E. Wilson, A basis for rational design of heat transfer apparatus, Trans. ASME 37 (1915) 47–70.
[30] A. Mansourizadeh, A.F. Ismail, Hollow fiber gas–liquid membrane contactors for acid gas capture: a review, J. Hazard. Mater. 171 (2009) 38–53.
[31] A. Gabelman, S.T. Hwang, Hollow fiber membrane contactors, J. Membr. Sci. 159 (1999) 61–106.
[32] V.Y. Dindore, D.W.F. Brilman, P.H.M. Feron, G.F. Versteeg, CO_2 absorption at elevated pressures using a hollow fiber membrane contactor, J. Membr. Sci. 235 (2004) 99–109.
[33] R.W. Baker, Membrane Technology and Application, John Wiley & Sons Ltd., England, 2004.
[34] K.Y. Wang, T. Matsuura, T.S. Chung, W.F. Guo, The effects of flow angle and shear rate within the spinneret on the separation performance of poly(ethersulfone) (PES) ultrafiltration hollow fiber membranes, J. Membr. Sci. 240 (2004) 67–79.
[35] A. Bottino, G. Capannelli, S. Munari, A. Turturro, High performance ultrafiltration membranes cast from LiCl doped solutions, Desalination 68 (1988) 167–177.
[36] T.S. Chung, J.J. Qin, J. Gu, Effect of shear rate within the spinneret on morphology, separation performance and mechanical properties of ultrafiltration polyethersulfone hollow fiber membranes, Chem. Eng. Sci. 55 (2000) 1077–1091.
[37] F. Tasselli, J.C. Jansen, F. Sidari, E. Drioli, Morphology and transport property control of modified poly(ether ether ketone) (PEEKWC) hollow fiber membranes prepared from PEEKWC/PVP blends: influence of the relative humidity in the air gap, J. Membr. Sci. 255 (2005) 13–22.
[38] M.C. Yang, E.L. Cussler, Designing hollow-fiber contactors, AIChE J. 32 (1986) 1910–1916.
[39] M. Mavroudi, S.P. Kaldis, G.P. Sakellaropoulos, A study of mass transfer resistance in membrane gas–liquid contacting processes, J. Membr. Sci. 272 (2006) 103–115.
[40] L.R. Fisher, R.A. Gamble, J. Middlehurst, The Kelvin equation and the capillary condensation of water, Nature 290 (1981) 575–576.